Changes in Thermal Structure of the Equatorial Pacific during the 1972 El Niño as Revealed by Bathythermograph Observations

A. E. GILL

Department of Applied Mathematics and Theoretical Physics, Silver Street, Cambridge CB3 9EW, England

(Manuscript received 1 March 1982, in final form 23 July 1982)

ABSTRACT

Bathythermograph data from the equatorial Pacific are used to study changes in upper ocean thermal structure during the period 1971–73 using data averaged over 2- or 3-month segments. This gives reasonable descriptions of the changes in two regions—the central Pacific (particularly in a section crossing the equator at 170–160°W) and along the eastern boundary. The behavior in the two regions is quite distinct, e.g., in the central Pacific, thermocline depth anomalies do not correlate well with surface temperature anomalies, but they do along the eastern boundary. The first baroclinic mode can be used to describe changes in vertical structure in the central Pacific, but the major changes near the eastern boundary are much more like those associated with the second baroclinic mode.

Subsurface changes along the eastern boundary are extremely large, e.g., the 14°C isotherm at the equator plunged from the 100 m level in January–February 1972 to the 250 m level in May–June. It did not get back to the 100 m level until the second half of 1973. The very large excursions are mainly within 10° of the equator, but the isotherm depth anomaly often had the same sign over the whole section from 20°S to 30°N.

Near the eastern boundary, the surface was nearly always anomalously warm when the thermocline was anomalously deep, but in the central Pacific there was not a strong relationship between surface temperatures and isotherm depth. In fact, the very large positive temperature anomaly found at 170–160°W during the September–November 1972 season occurred when the 20°C isotherm was shallower than normal.

1. Introduction

The large interannual changes of sea-surface temperature in the equatorial Pacific and their effect on the atmosphere (Bjerknes, 1966a, 1969; Horel and Wallace, 1981) are well known, but relatively little is known about the associated subsurface changes. This paper represents an attempt to find out something about subsurface changes in thermal structure using the available bathythermograph records. A detailed description of the surface temperature changes has been given by Rasmusson and Carpenter (1982) who also review earlier work. The El Niño phenomenon is associated with "warm events" which first show as anomalously warm surface waters off the South American coast at the beginning of the year. This positive anomaly may last for 14 months. The region of positive anomalies is found to spread westward along the equator (Hickey, 1975) and by the end of the El Niño year, most of the region from 160°E to the coast is anomalously warm. The meridional extent of the warm region is ±10° of latitude at the dateline increasing to ±20° from 150°W to the eastern boundary. The accompanying changes in surface winds are also described by Rasmusson and Carpenter (1982). Surface salinity and temperature changes are discussed by Hires and Montgomery (1972), Wooster and Guillen (1974) and Donguy and Henin (1978, 1980), while Henin and Donguy (1980) discuss changes in heat content.

Information on subsurface changes near the equator and along the eastern boundary is much more sparse, and often in internal reports and workshop proceedings rather than in readily available journals. Austin (1960) described changes in subsurface structure during the 1957 El Niño between 140 and 150°W and these are also described by Bjerknes (1966b). Wyrtki *et al.* (1977) describe subsurface changes based on 27 transequatorial sections made between 1972 and 1975; 11 sections crossed the equator at 153–154°W, 13 at 165–167°W and the other three at 125°W, 139°W and 140°W. Wyrtki (1975), in discussing the causes of El Niño, described subsurface changes along the South American coast associated with the 1972 El Niño. A more comprehensive description of these changes is given by Wooster and Guillen (1974), Zuta *et al.* (1980), Enfield (1981) and Robles *et al.* (1980).

The information given in this paper is mainly descriptive and based on the available BT data in the tropical Pacific up to 1973. Attention is particularly directed to the zone corresponding to the equatorial and coastal waveguides, that is, along the equator and along the eastern boundary. Theoretical discussion

0022-3670/82/121373-15$07.75

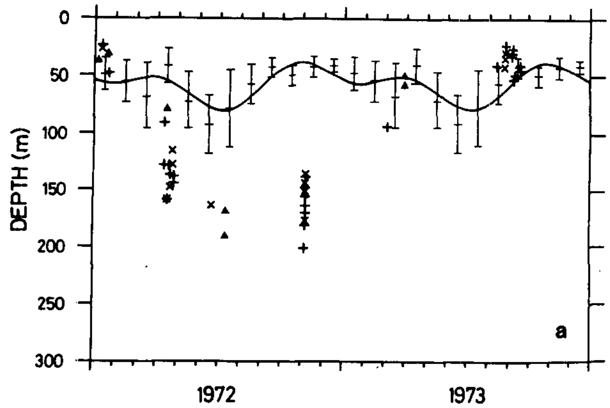

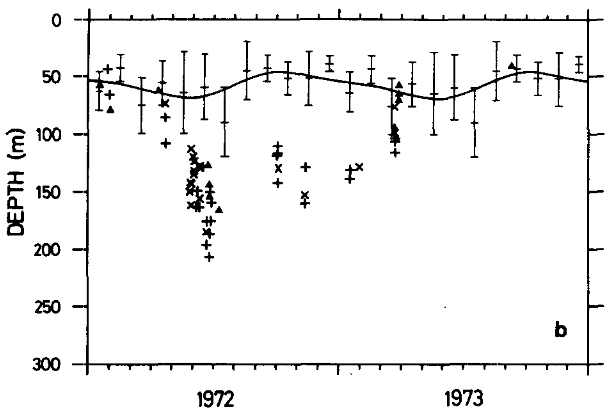

FIG. 1. Depth of the 16°C isotherm at the equator (2°S–2°N) during 1972 and 1973 for (a) 85–80°W, (b) 85–90°W. Product signs represent data between 2°S and 1°S, plus signs 1°S–1°N and triangles 1°N–2°N. The solid lines show seasonal changes for all data in the years considered as non-El-Niño years, i.e., 1944, 45, 50, 52, 54, 55, 56, 59, 60, 61, 62, 64, 67, 68, 71. These lines are least-squares fits to an annual plus semi-annual wave while the range markings show monthly means and standard deviations.

is limited to a brief examination of the relation between sea-level and isotherm displacements. A later paper will be concerned with using theory to reconstruct water movements during the 1972 El Niño and hence with explanation of the observed changes.

2. The bathythermograph data

The data used was kindly made available by Dr. Gary Meyers (see Meyers, 1979) and consists of a merged set of mechanical and expendable bathythermograph data for the Pacific Ocean between 30°S and 30°N. The data begin in the 1940's and continue to the end of 1973. It is extremely patchy in both space and time, so the usefulness for studying interannual variability is rather limited. Of the El Niño events which occurred during the period covered by the data, the one for which most information is available is the 1972 event, so this paper is almost entirely concerned with that event. Scraps of information are available about other events, but the coverage is so poor compared with 1972 that it was not considered worthwhile to look at these in detail.

The changes where the equator meets the eastern boundary are very large during El Niño events, and Fig. 1 illustrates this by showing, for 1972 and 1973, changes in depth of the 16°C isotherm in two adjacent 4° × 5° rectangles centered on the equator. Note that although there is a large scatter in the data collected in any single month, one can have confidence that the anomalies are real 1) because the changes in the two adjacent regions are quite similar and 2) because the displacements at the height of the event are a large number of standard deviations outside the "normal" range. In order to obtain the "normal" seasonal cycle, data from years considered as anomalous were excluded from the data sets and means and standard deviations computed for the remaining 15 years of data. Also shown is a least-squares fit to the same 15 years data of an annual plus semiannual cycle.

For studying the anomalies, averages will be taken to remove the scatter seen in Fig. 1. However, it is of interest to comment on the source of this scatter as the BT set combined some interesting information which is pertinent. Two periods were selected where high resolution in time was obtained in a small area, and the changes observed at these times are shown in Figs. 2 and 3. Fig. 2 shows that internal tides can be quite important as the 16°C isotherm moved over a depth range of 30 m at 2°S, 83.3°W on 20 August 1966 with changes which fit a tidal cycle quite well. Fig. 3 shows the changes observed in a 3° square where a large number of measurements were made in the same month. Here it is hard to pick out a coherent pattern and it is interesting that the range of depths (50 m) for the 12°C isotherm is much greater than the range (25 m) for the 16°C isotherm. The reason for this is unknown. Little more about such short-time variability can be found from the BT record, but more information is available (e.g., Wyrtki *et al.*, 1981; Huyer, 1980).

Spatial smoothing will also be applied in studying anomalies because all observations in some fairly large rectangles are sometimes used to obtain averages. Hence it is of some interest to look at the data file for cases where good spatial sampling is available. Fig. 4 gives an example with relatively good spatial resolution. This shows all the measurements of 16°C isotherm depth made in May 1958 within 2° of the equator. The solid line is the "normal" May curve calculated from the May observations made in the 15 "normal" years referred to above. The 1958 values show coherent variations about the mean with a superimposed scatter having a range of about 20 m. Other such sections are discussed by Halpern (1980).

Because of this scatter, a single measurement does not give a reliable indication of mean conditions, but it is found that if averages are taken over suitable space-time bins, the fields obtained show reasonable

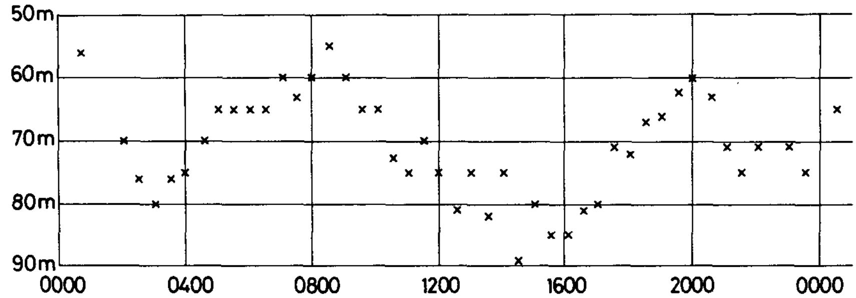

FIG. 2. Depth of the 16°C isotherm at 2°S, 83.3°W on 20 August 1966.

smoothness over many such bins. The time bins usually need to be two or three months to give the best compromise between having sufficient data and being able to describe significant seasonal and non-seasonal changes. Spatial bins were generally 5–15° in longitude and 2–4° in latitude. The best coverage of the near-equatorial regions was in the coastal strip along the eastern boundary with distributions in time like that shown in Fig. 1 being somewhat better than found in the sixties. Data density within this strip is rather better north of Panama and along the coast of Peru than elsewhere. The coverage between 170 and 160°W near the equator is as good as in the coastal strip in the seventies, but not before, and elsewhere along the equator there is generally very little use for describing non-seasonal changes. Thus the description of subsurface changes in this paper is mainly restricted to the period 1971–73, to the coastal strip, and a section crossing the equator at 170–160°W. A few other pieces of information are given where available.

3. Changes near the eastern boundary in the period 1971–73

a. Time series at the equator

Fig. 5 shows time series of isotherm depth and surface temperature averaged over the region 2°S–2°N

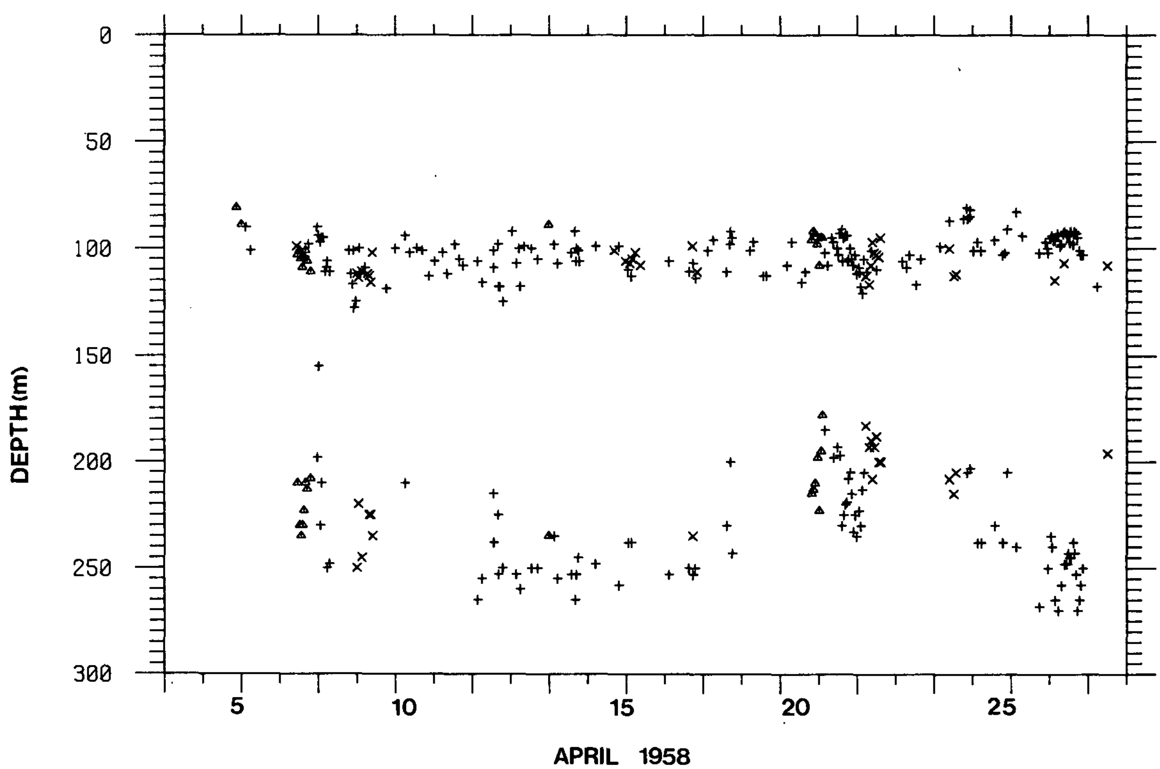

FIG. 3. Depth of the 20°C isotherm (points above 140 m depth) and of the 12°C isotherm (points below 140 m) in the 3° square 141.5 to 138.5°W, 1.5°S to 1.5°N during April 1958. Product signs are in the southernmost third of the squares, plus signs in the central third and triangles in the northern third.

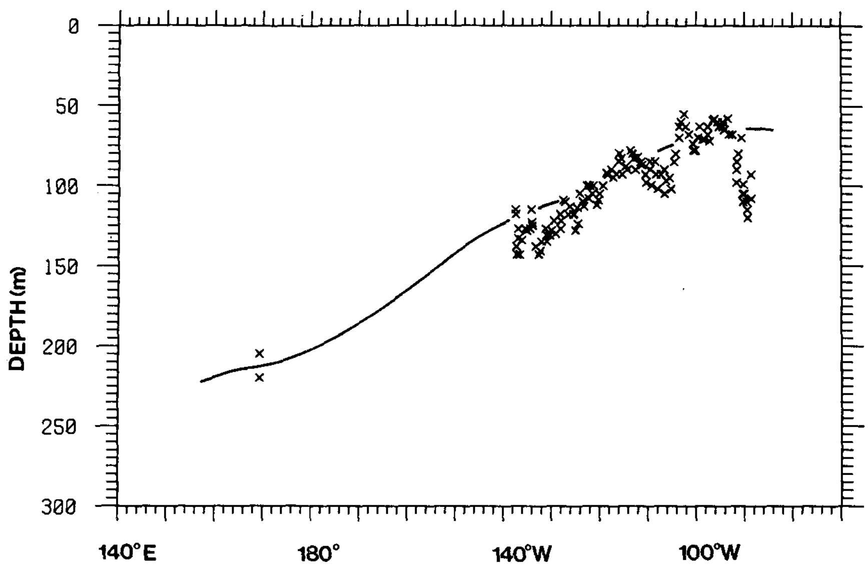

FIG. 4. Measurements of depth of the 16°C isotherm (crosses) made in May 1958 between 2°S and 2°N. The solid line shows the normal position of this isotherm during May.

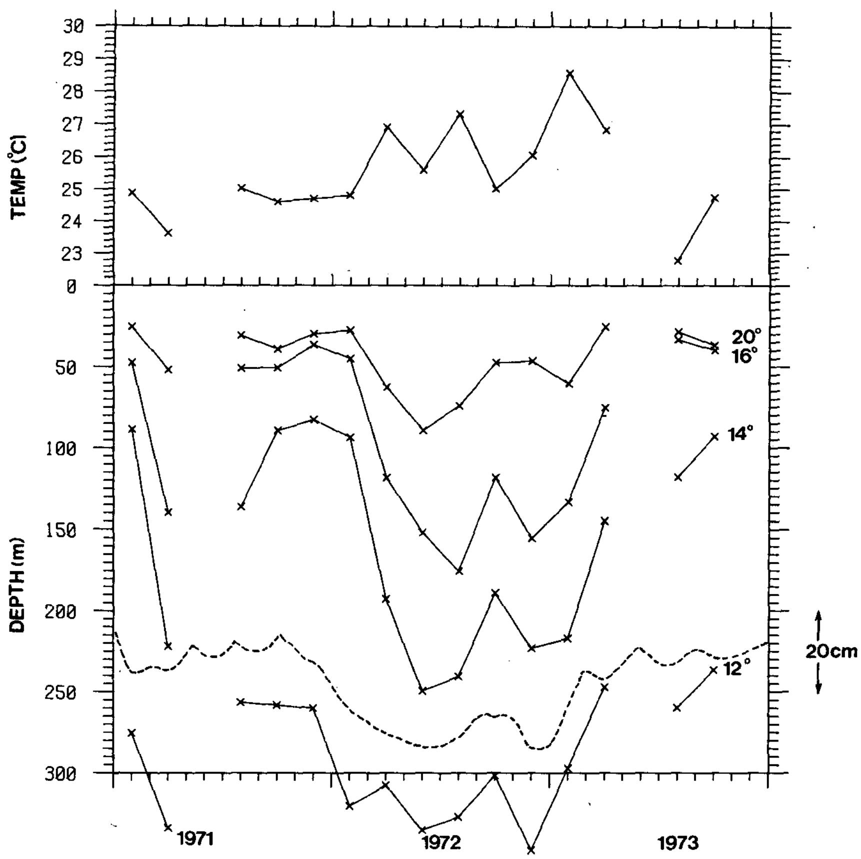

FIG. 5. Surface temperature (upper panel) and isotherm depths (lower panel) as functions of time at 80–95°W, 2°S–2°N. Points marked are averages using all BT's in the designated area for a two-month period. The dashed lines show sea level (positive downward) at Baltra Galapagos Is. (0.4°S, 90°W).

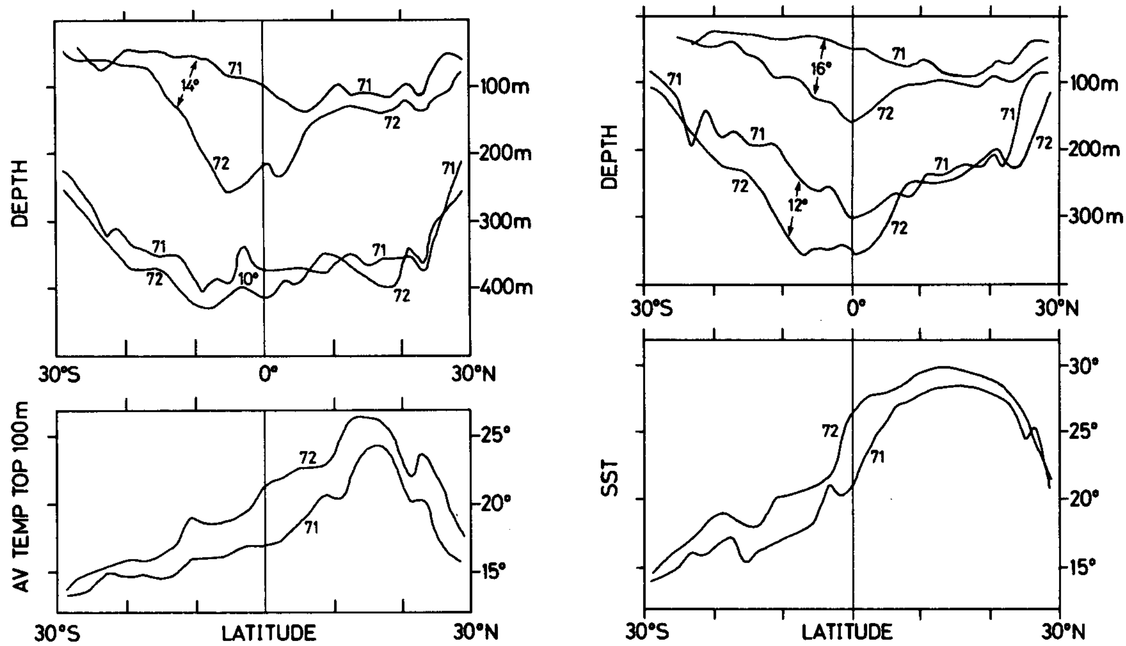

FIG. 6. Latitude-depth and latitude-temperature sections along the eastern boundary of the Pacific, showing comparison between the three-month periods September–November for 1971 and 1972. Quantities shown are the depth of the 10, 12, 14 and 16°C isotherms, the average temperature of the upper 100 m, and the sea-surface temperature.

near the eastern boundary (95–80°W). Data points represent two-month averages for all BT's in the area. The dominant feature is the plummeting of the isotherms to extraordinarily large depths starting at the beginning of 1972. The isotherms reach a maximum depth around May, then shallow for a few months before reaching another maximum around December. There is a rapid recovery in the first few months of 1973. The same behavior can be seen in the inverted Galapagos sea level which is also shown in the figure. The first peak in May and June 1972 is 22 cm above the level for November 1971 while the second peak in December is slightly higher. The 14°C isotherm is the one showing the greatest excursions, its maximum depth in May–June 1972 being 170 m more than the depth in November–December 1971. The second maximum at the end of the year is not so deep. These changes can also be seen in the hydrographic sections across the equator at 82–83°W from 1.5°N to 3°S made quarterly during 1972 and 1973 and displayed by Enfield (1981). He showed that the largest temperature changes are at the 60 m level where the temperature in November–December 1971 was 14°C but had risen to 22–23°C the following year, i.e., an 8–9°C increase!

The hydrographic sections also show a strong frontal structure in the top 30 m, whereas there appear to be no systematic gradients at lower levels. This gives rise to a large scatter in surface temperature, values of which may be aliased according to the position of observation. Nevertheless, the warming in 1972 can be seen in the averages plotted in Fig. 5.

b. Changes along the eastern boundary

A coastal strip was defined as the region between the boundary and the line linking the points 30°N, 118°W; 20°N, 110°W; 5°N, 81°W; 4°S, 85°W; 20°S, 73°W; and 30°S, 73°W, and data within this zone were put into bins covering 2° of latitude and three months in time. Data in each bin were averaged and used to produce Figs. 6 and 7. The anomalies shown in Fig. 7 are relative to the average of *all* data, not just the non-El-Niño years referred to in the caption to Fig. 1 (the word "anomaly" is used in this sense throughout). There was good coverage (i.e., very few empty bins) in September–November 1971, when conditions were close to normal, and for the corresponding period the following year, when conditions were strongly anomalous. Fig. 6 shows the comparisons. The 14°C isotherm shows the largest displacement, and both 14°C and 16°C isotherms are lower in 1972 over practically the whole section. The displacement of the 10°C isotherm is much less. As a result of these displacements, the average temperature of the upper 100 m was considerably higher in 1972, the change being about 3 K between 10°S and 10°N. The surface temperature was also higher in 1972, but by a smaller amount.

Another way of displaying the data is in terms of

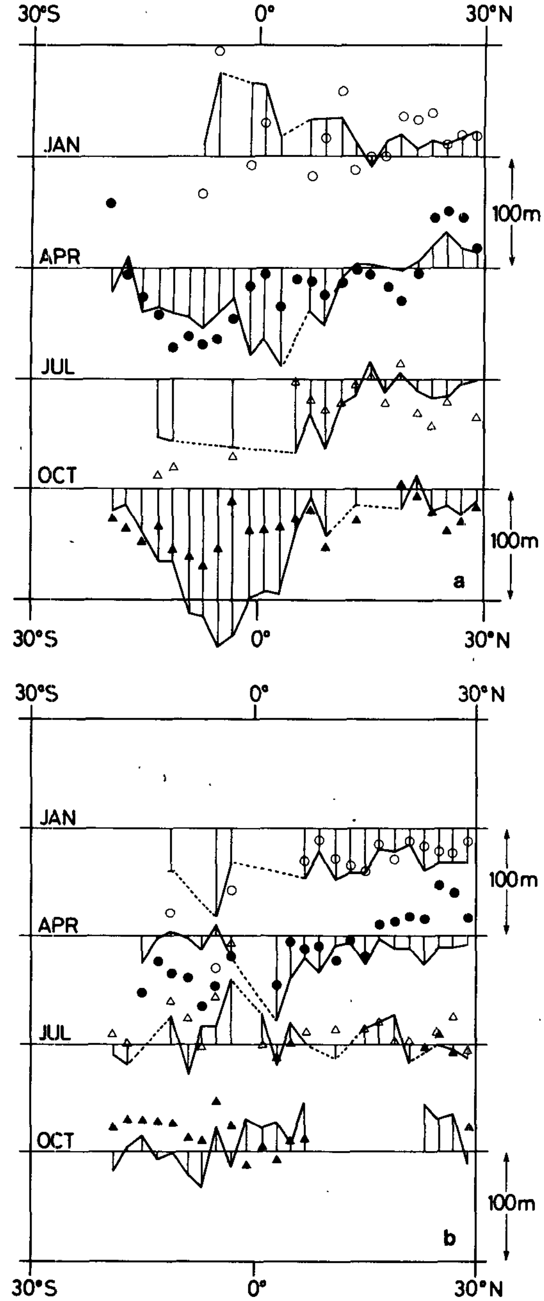

FIG. 7. Anomaly in depth of the 14°C isotherm (solid line and vertical bars) along the eastern boundary of the Pacific for successive three-month seasons in (a) 1972 and (b) 1973. *Positive* values correspond to *upward* displacements. Each season is labelled by the middle one of the relevant three months. Also shown is the surface temperature anomaly. Different symbols are used for each season to prevent confusion where the curves cross. The scale marked 100 m corresponds to 4.5 K for the temperature anomaly curves. Positive anomalies are drawn *downward* to emphasize the correlation between a warm surface and a deep isotherm.

anomalies from the long-term mean for each season, as is done in Fig. 7 for both isotherm depth and surface temperature. Here the development of the anomaly from season to season can be seen for a period of two years. Note that there is a good correlation between isotherm depth anomaly and surface temperature anomaly in that the surface is usually warmer when the 14°C isotherm is deeper than average. There are, however, some exceptions and the strength of the temperature anomaly does not always relate well to the strength of the depth anomaly. There are little data in the BT file south of 20°S, but there are some hydrographic data between 18 and 27°S inshore of 73°W given by Robles *et al.* (1980). They found that in the winter (June–August) and spring (September–November) of 1972, sigma-*t* surfaces were deep and surface waters were warm and saline compared with normal. They also found that subtropical surface water extended much further southward along the coast than normal.

Hydrographic data are also available between 1.5°N and 18°S for comparison with the BT results, although not in the form of anomalies. Zuta *et al.* (1980) give temperature and salinity sections along the coast for this range of latitudes for November 1971, February–March 1972 and August–September 1972. The temperature sections are also given by Enfield (1981) and the same changes as seen in Fig. 6 may be discerned. Zuta *et al.* (1980) also give depth-time plots of temperature and salinity for the coastal areas around 6, 9, 14 and 18°S. The first two show similar changes to those seen in Fig. 5 but at 14°S, the 14°C isotherm was still shallow (30 m) in February 1972. In March–April it was much deeper, indicating that the drop occurred here later than at the equator. This is consistent with the idea that isotherm depth changes propagate poleward in the same way as coastal sea level changes (Enfield and Allen, 1980; Chelton, 1981). The data in Fig. 7 also give indications of poleward propagation of anomalies. For shorter period changes, poleward propagation is well established from measurements by Smith (1978) and the associated offshore structure of the variations has been identified by Huyer (1980).

Some information about the offshore scale of longer period changes can be obtained from the topography of isotherms or isopycnals along the coastal strip, maps being given by Wyrtki (1975), Zuta *et al.* (1980), Robles *et al.* (1980) and Enfield (1981). Details of the patterns are rather complicated, but maps such as those of Enfield (1981) of differences in depth between a warm year (July 1976) and a normal year (August 1971) indicate an offshore scale of around 150 km off Peru with a tendency for larger scales to the north. The scales in northern Chile (Robles *et al.*, 1980) appear to be somewhat less, e.g., a comparison of the topographies of the 26.4 sigma-*t* surface in the winter of 1972 compared with 1967 indicates a value of about 50 km.

These results, and those shown in Fig. 7, are interesting from the point of view of models of the

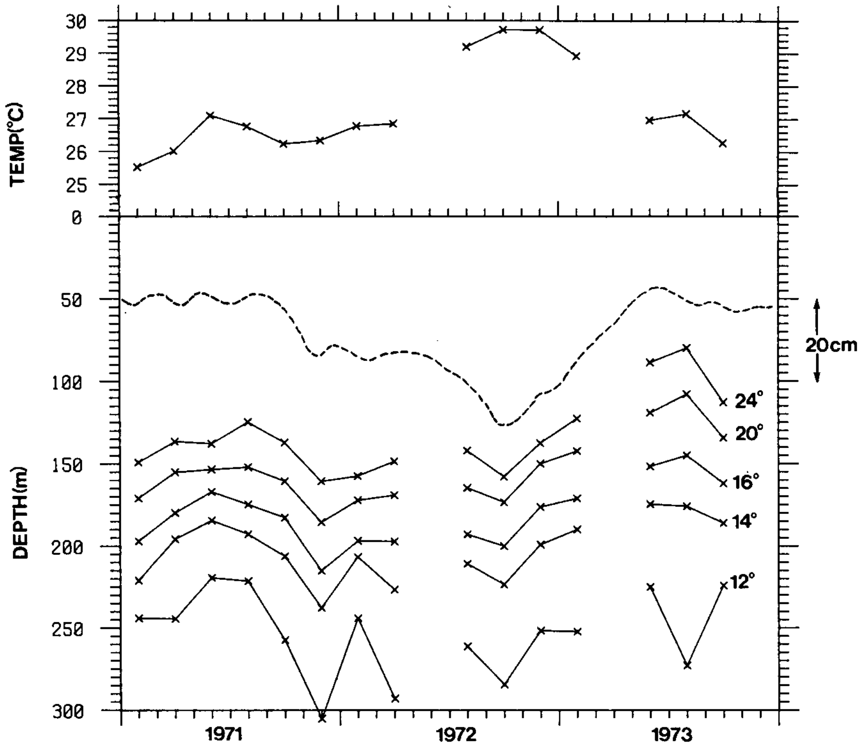

FIG. 8. Surface temperature (upper panel) and isotherm depths (lower panel) as functions of time at 160–170°W, 2°S–2°N. Points marked are averages using all BT's in the designated area for a two-month period. The dashed lines are sea-level at Christmas Is. (2°N, 157°W) on the left side, and at Canton Is. (2.8°S, 172°W) on the right side. These gauges only operated during the time shown. The curves are both shown relative to a common zero representing the long-term mean value in each case.

ocean, which often have a vertical boundary at the eastern edge. In such models anomalies found at the equator propagate quickly poleward in the form of coastal Kelvin waves so events at the equator would be repeated at 30° latitude at a time of order a month later.

The offshore scale in the models decreases rapidly with distance poleward. For shorter periods (a month or less), the scale is that associated with the Kelvin wave, namely the Rossby radius (see, e.g., Gill, 1982). For a mode with a propagation speed of 1 m s^{-1}, this scale is 40 km at 10° latitude and 14 km at 30° latitude. For longer periods, the scale is larger because anomalies propagate westward at the long planetary wave speed which falls off rapidly with latitude. For a 1 m s^{-1} mode, the distance propagated in a season (3 months) is 300 km at 10° latitude and 35 km at 30° latitude.

In the models with a vertical boundary, anomalies in isotherm depth associated with longer time scale (i.e., longer than the time for a Kelvin wave to propagate 30°, say) changes become uniform with distance along the coast in order to satisfy the thermal-wind equation, i.e., no horizontal temperature gradient anomaly is allowed, or there would be a vertical gradient of onshore velocity anomaly. In practice, Fig. 7 shows that the isotherm depth anomaly is not uniform but is much smaller poleward of 20° than it is near the equator. The change in amplitude could be partly due to the averaging procedure since the offshore scale of the anomaly decreases with latitude, but this does not seem likely to be the sole explanation. An important factor in practice could well be the effect of the continental slope as demonstrated in the model of Sugonihara (1981). In that model, much of the Kelvin wave energy was transferred to barotropic motion at about 20° of latitude and then radiated westward in the form of barotropic Rossby waves.

4. Changes at 170–160°W during 1971–73

a. Time series at the equator

The zone with the most data in the central Pacific on the equator during 1971–73 was at 170–160°W, which is where the ship track from Hawaii to Samoa crosses the equator. There is also reasonable data coverage at 160–150°W for the second half of this period, but details are not given as the changes are similar to those at 170–160°W.

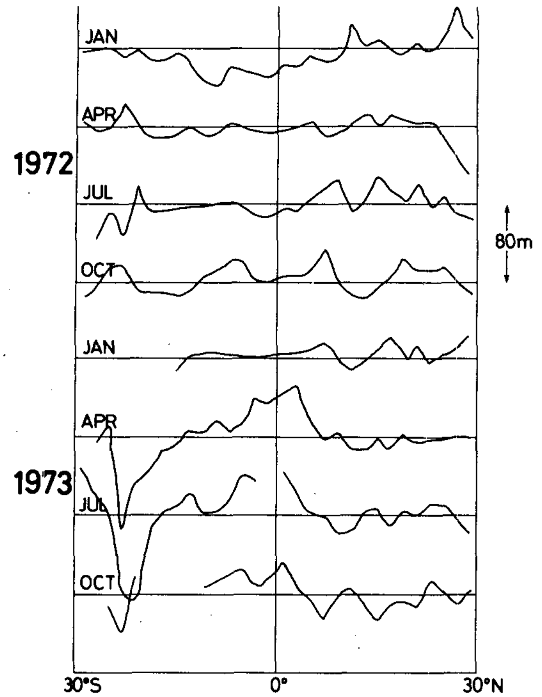

FIG. 9. Anomalies in depth of the 20°C isotherm along the strip which is 10° of longitude wide and runs from 30°S, 175°W to 30°N, 155°W. The curves are based on averages of all values in 2° latitude bands and three-month seasons centered on the months shown. *Positive* values indicate *upward* displacement.

Fig. 8 shows time series at the equator (2°S–2°N averages over 2 month intervals) of isotherm depths and surface temperature. In 1971 the changes in isotherm depth are not dissimilar from those for a normal year with the thermocline about 30 m deeper toward the beginning and the end of the year. In mid 1972 the isotherms are a little deeper than normal but the most spectacular change is in 1973 when the thermocline rises to much higher levels in the middle of the year. The same rise occurs at 160–150°W and coincides with a large drop in sea level at Canton Island. The changes are not so obvious from the sections presented by Wyrtki *et al.* (1977) because there are considerable changes in the mean depth of the isotherms over the large range of longitudes involved.

The most spectacular changes in 1972 are not those in isotherm depth, but those in surface temperature which was about 3 K higher than normal in the second half of the year. These are the surface temperature changes which have such profound effects on the atmosphere (Horel and Wallace, 1981; Rasmusson and Carpenter, 1982).

b. Changes along a meridional section

Good data coverage was found in a strip crossing the equator at 170–160°W and running slightly east of north. The strip was defined by lines joining 30°S, 180°W to 30°N, 160°W and 30°S, 170°W to 30°N, 150°W, and includes the Hawaii–Samoa ship track. Fig. 9 shows anomalies in the depth of the 20°C isotherm along this track for 1972–73, while Fig. 10 shows anomalies in surface temperature. Note that high surface temperatures do *not necessarily* coincide with a low thermocline or low-surface temperature with a high thermocline. For instance, the high temperature anomaly in October 1972 occurs when the 20°C isotherm was at its normal level, while the high thermocline in April 1973 coincided with the surface being on the warm side. Note also the large depression of the isotherm depth near the Tropic of Capricorn in April and July 1973, which does not have a matching surface temperature signature.

The anomaly diagrams (Figs. 9 and 10) give an impression of the horizontal scale of the anomalies. The meridional scale for the isotherm depth anomalies centered on the equator matches that for equatorially-trapped waves quite well, e.g., the first mode Kelvin wave has amplitude falling from its peak value at the equator to about 20% at ±6° latitude and matches the anomaly for April 1973 quite well. The first planetary wave has peak elevation at about 4° latitude and falls to 20% of this value at about 8° latitude. The scales for surface temperatures are similar to those of the waves, or perhaps a little bigger if the large October 1972 anomaly is taken as the prime example. Coherence over distances of around

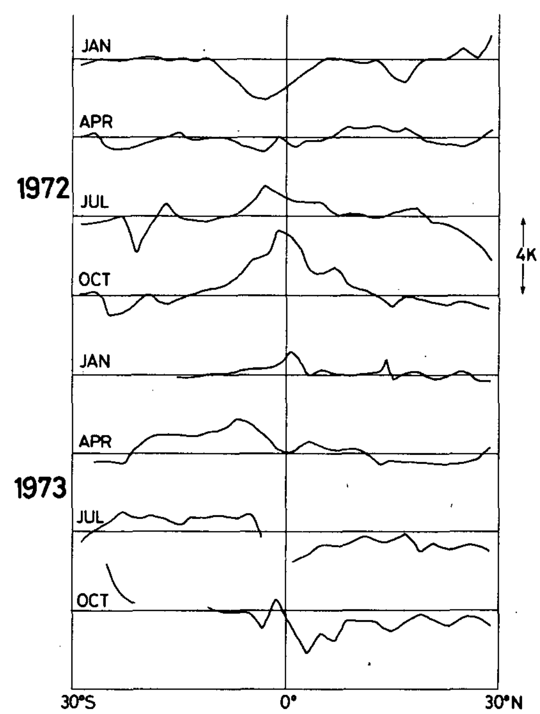

FIG. 10. Anomalies in sea-surface temperature corresponding to the depth anomalies shown in Fig. 9, and computed by the same method. *Positive* values correspond to *warm* anomalies.

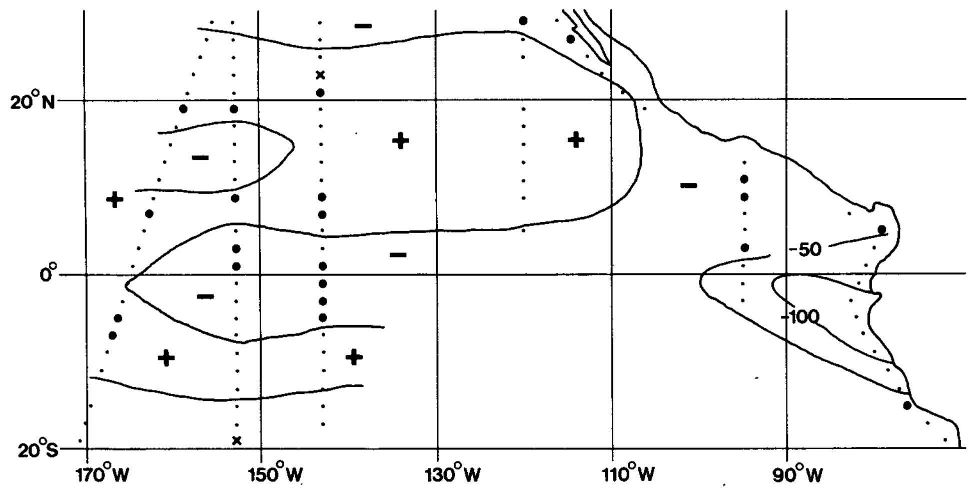

FIG. 11. Anomaly in depth of the thermocline during the three-month period September–November 1972. The map is based on six cross-equatorial sections. One is the coastal section already described. The others are strips 10° of longitude wide and centered on the data points shown. The isotherm selected to represent the thermocline was 14°C for the two eastern sections, 16°C for the 120°W section, 18°C for the 143°W section, and 20°C for the two western sections. The dots represent data points, large dots denoting where the value was between 20 and 50 m. The two product signs are the only data points where the values disagree with the contouring.

±10° have also been found in variability with periods of 2 or 3 months (Barnett and Patzert, 1980).

5. Changes at other longitudes

There was very little information in the data file about changes west of the data line during 1971–73. However, some information on the general character of the interannual variability in the zone can be obtained from the study of White and Hasanuma (1980), and from Wyrtki (1979)'s study of sea-level changes during the 1976 El Niño and from studies of the 137°E section (Masuzawa and Nagasaka, 1975). In particular, White and Hasanuma (1980) found empirical orthogonal functions to describe interannual temperature variability along the 155°E section and dynamic height changes over the whole area between the equator and 35°N, the dateline and the western boundary. In the case of temperature, the main variability was at the thermocline depth and extended to about 15°N. In the case of dynamic height, the empirical function most closely associated with El Niño events extended along the equator from the western boundary to about 175°E, with a meridional scale varying between 5° and 10° of latitude.

Information from longitudes between 150°W and the eastern boundary is also rather sparse, so it was decided to concentrate attention on six cross-equatorial sections along which data coverage was sufficiently dense. Data along these sections were arranged in three-month seasons and 2° latitude bins. Very often there would be no information in a bin, but the coverage for September–November 1972 was exceptional and Figs. 11 and 12 show results for this season.

Fig. 11 shows the general character of the thermocline depth anomaly field for September–November 1972. The region of depressed thermocline runs along the equator to 160°W with a meridional scale of ±5° at 143°W and 153°W, broadening considerably as the eastern boundary is approached. This is typical of the behavior found in models such as those of Anderson and Rowlands (1976), Hurlburt *et al.* (1976), McCreary (1976), Cane and Sarachik (1979), Philander and Pacanowski (1980) and O'Brien *et al.* (1981). The depression is very much greater near the eastern boundary. The scatter diagram of observed 14°C isotherm depths along the equator (Meyers, 1979, Fig. 1) indicates that the very large depressions do not extend west of 100°W, so are probably confined to the region bounded by the −50 contour in Fig. 11. The figure also shows a large area, where the thermocline is shallower than normal, this region extending to about 27°N.

Fig. 12 shows information on the thermal structure from three of the sections, comparing the September–November 1972 conditions (broken lines) with the seasonal mean. The upper curve is the sea surface temperature and the lower curve the average temperature of the top 100 m.

At 95°W, the two curves are well separated because the mixed-layer depth is much less than 100 m, and so changes in the average temperature over the top 100 m tend to reflect vertical movements of the thermocline rather than changes in temperature of the mixed layer. In the central Pacific sections, the two curves often coincide, showing that the mixed layer is over 100 m in depth. The region near 10°N, where

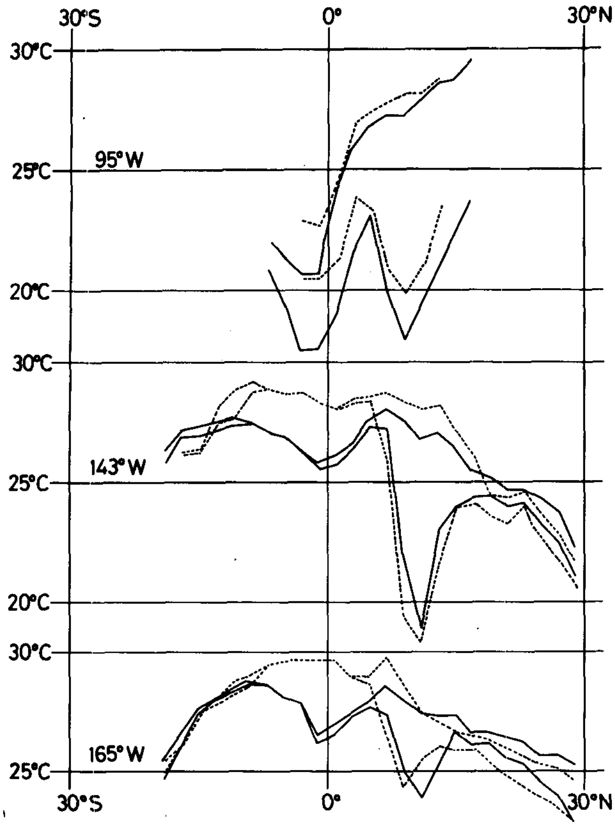

FIG. 12. Sea-surface temperature (upper curves) and average temperature over the upper 100 m (lower curves) for three cross-equatorial sections for the three-month season September–November. The solid lines are mean curves for this season while the dashed lines are for 1972. The curves are based on points representing means of all data in a 10° longitude by 2° latitude area for the three-month period. The two sections labelled 95°W and 143°W are meridional sections centered on the indicated longitude, whereas the third section is the same as in Fig. 9.

the mixed layer gets much thinner, shows up very prominently, and this is due to upwelling associated with Ekman convergence below the intertropical convergence zone. In normal years, the temperature at the equator is cooler than at 5° to the north or south due to the combined effects of advection from the east by the South Equatorial Current and of upwelling. The interesting feature of the 1972 conditions in the central Pacific is that the equatorial dip in surface temperature has disappeared, and very warm water is found at the equator. The temperatures are in fact higher than normally found anywhere in these sections.

6. Changes in vertical structure

It is also interesting to look at vertical temperature profiles and the way they change. Such profiles were constructed first by plotting all observations of isotherm depth and surface temperature in a 10° wide longitude band between 2°S and 2°N, and during a selected period (usually two months) on a temperature-depth plot giving a scatter diagram from which mean profiles could be constructed. In the pictures these have been reduced to show means and standard errors only.

Fig. 13 shows the changes at the equator near the western boundary between 140 and 150°E. There is little data available on the equator west of the date line, apart from occasional patches such as those which have allowed Fig. 13 to be constructed. The figure shows that the thermocline was about 50 m higher in September–October 1972 than in September–October 1971 at this location, in contrast to the east Pacific, where the thermocline was abnormally low. This is consistent with sea-level measurements reported by Wyrtki (1977) [e.g., at Anewa Bay, Solomon Islands, the sea level was about 23 cm lower in September–October 1972 than the year before].

Fig. 14 shows two examples of the changes which take place between 160 and 170°W. Fig. 14a shows a rather rapid drop in the thermocline which took place toward the end of 1971. Since it occurs a couple of months prior to the drop at the eastern boundary it could be associated with a Kelvin wave propagating toward the eastern boundary and thus represent a precursor to El Niño. However, this interpretation is not certain because the seasonally averaged data give a drop of about 30 m at this time of year, and the 1971 change is not significantly different from that. It is interesting, nevertheless, to plot the vertical displacement of each isotherm as a function of the mean depth of that isotherm. This gives the displacement-depth curve shown on the right and indicates that the displacement varies linearly with depth. Fig. 14b compares the November–December 1971 profile with the corresponding one a year later. This vividly illustrates how surface temperature changes need *not* correlate with isotherm displacement since the thermocline was much higher in 1972 when the surface was warmer.

Fig. 15 shows temperature profiles at the equator near the eastern boundary between 90 and 80°W. Fig. 15a shows the change in a period of rapid change, one profile for the period January–February 1972, and the other for the period between the beginning of May and the middle of June 1972. The right-hand panel shows the displacement h of each isotherm as a function of its mean depth. The profile is quite different from that found in the central Pacific (see Fig. 14a) in that a change of sign in $\partial h/\partial z$ occurs in the upper 300 m. Fig. 15b compares profiles for November–December 1971 and November–December 1972, showing the changes over a full year.

It is interesting to try and relate the displacement-depth curves shown in Figs. 14a and 15a to theory. Many of the models consider only one vertical mode, so it is useful to calculate the displacement-depth curves for the first baroclinic mode infinitesimal dis-

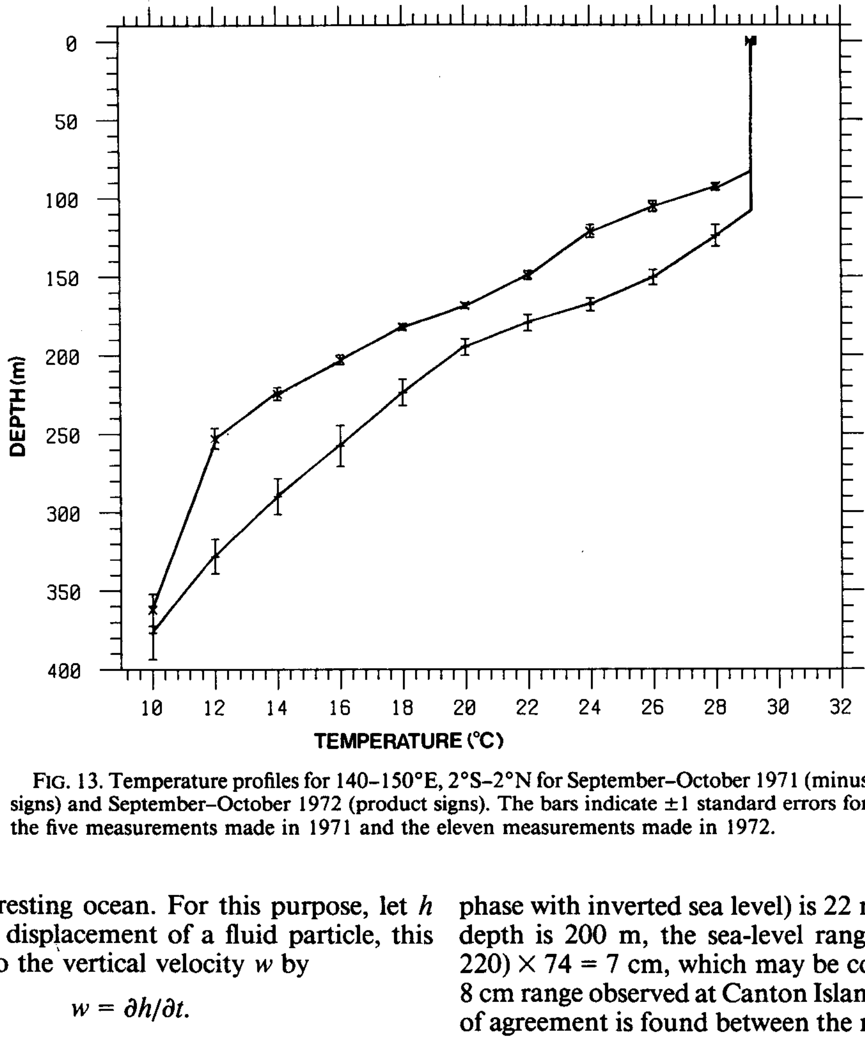

FIG. 13. Temperature profiles for 140–150°E, 2°S–2°N for September–October 1971 (minus signs) and September–October 1972 (product signs). The bars indicate ±1 standard errors for the five measurements made in 1971 and the eleven measurements made in 1972.

turbance to a resting ocean. For this purpose, let h be the vertical displacement of a fluid particle, this being related to the vertical velocity w by

$$w = \partial h/\partial t.$$

The vertical scale of the first baroclinic mode is large compared with the 300 m over which the profiles in the figures extend, so $\partial h/\partial z$ is approximately constant over this depth range. The relationship between $\partial h/\partial z$ and surface elevation η at the surface is simply (see Appendix)

$$\frac{\partial h}{\partial z} = \frac{\eta}{H_e}, \tag{1}$$

where H_e is the equivalent depth equal to the square of the wavespeed divided by the acceleration due to gravity. In the central Pacific, the wave speed is about 2.6 m s^{-1} (Wunsch and Gill 1976), so H_e is about 74 cm. Fig. 14a shows that $\partial h/\partial z$ is about $1/7$, so the corresponding sea-level change should be 11 cm. At the nearest tide gauge [Canton Island (2°48′S, 171°43′W)], the average sea level for November–December 1972 was 9 cm below that for October, which is in reasonable agreement with (1). The seasonal changes given by Meyers (1979, Fig. 4) are also in agreement with (1). Between 180 and 160°W the range of the 14°C isotherm depth (which varies in phase with inverted sea level) is 22 m. Since its mean depth is 200 m, the sea-level range should be (22/220) × 74 = 7 cm, which may be compared with the 8 cm range observed at Canton Island. The same level of agreement is found between the range of the 14°C isotherm depth at 140–160°W and the range of sea level at Christmas Island (1°57′N, 157°28′W).

Although the principal changes at 170–160°W appear to be associated with the first baroclinic mode, it is clear from Fig. 8 that a single mode cannot describe all the changes. For instance, the spacing between the 14 and 24°C isotherms varies between 50 and 95 m, whereas it would vary rather little if only the first mode were present. Such changes in spacing can occur if a second mode is also involved and are associated with the strength of the equatorial undercurrent (Gill, 1975). Another significant factor is the large change of dynamic height associated with temperature changes in the mixed layer. If this change is δT, if H_{mix} is the mixed-layer depth and α the thermal expansion coefficient, then the dynamic height change is that associated with the thermal expansion, namely

$$\alpha H_{mix} \delta T.$$

For $\alpha \approx 3.2 \times 10^{-4}$ K^{-1} and $H_{mix} \approx 100$ m, the surface is raised 10 cm when the mixed-layer tem-

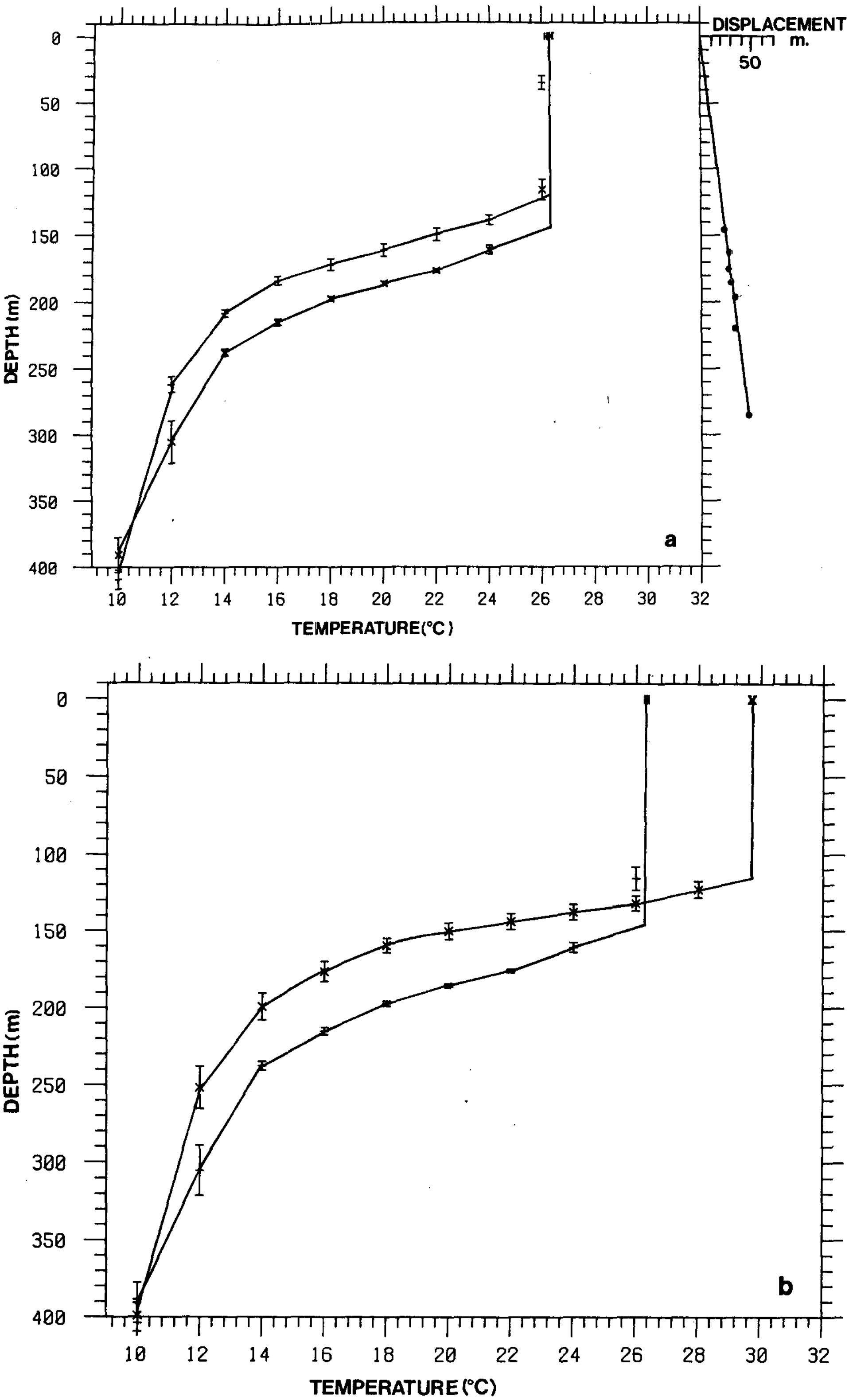

FIG. 14. Temperature profiles for 170–160°W, 2°S–2°N. In (a) the profile for October 1971 [nine measurements (minus signs)] and November–December 1971 [11 measurements (product signs)] are compared, and the panel on the right shows the displacement of each isotherm in this period as a function of its mean depth. The estimate of the mean depth of the 10°C isotherm for November–December is unreliable as only eight of the 11 profiles reached the 10°C level. In (b) the November–December 1971 profile is compared with the profile for November–December 1972 (based on seven measurements marked by product signs). The bars show standard errors.

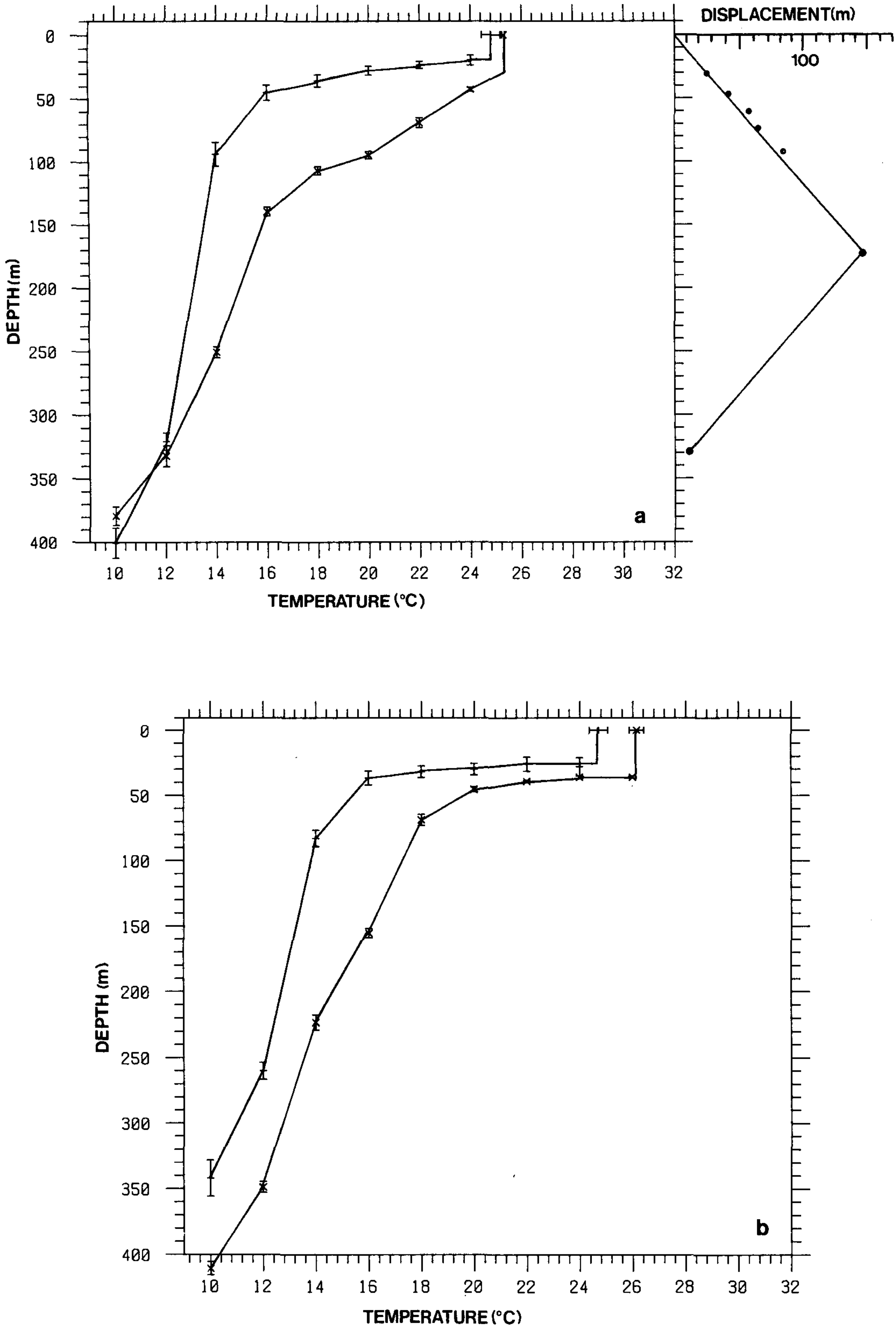

FIG. 15. Temperature profiles for 90–80°W, 2°S–2°N. In (a) the profile for January–February 1972 [nine measurements (minus signs)], is compared with that about 100 days later for the period 1 May–15 June 1972 [18 measurements, (product signs)]. The panel on the right shows the displacement of each isotherm in this period as a function of its mean depth. The estimate of the mean depth of the 10°C isotherm for January–February is unreliable as only five of the nine bathythermographs reached the 10°C level. In (b) the profile for November–December 1971 [four measurements (minus signs)], is compared with that for November–December 1972 [21 measurements (product signs)]. The bars indicate standard errors.

perature is increased by 3 K. The usual normal modes cannot describe such a change because small perturbations to an ocean with undisturbed temperature a function of depth only produce zero temperature change at the surface. Thus to obtain surface changes, either heat inputs across the upper boundary are required or the undisturbed state must contain horizontal temperature gradients. Then horizontal advection produces temperature perturbations.

Near the eastern boundary, the picture is quite different as $\partial h/\partial z$ has the extraordinarily large value of 0.9 in Fig. 15a. The sea level at Baltra rose by 10 cm during this period, so if (1) is applied, despite the fact that linear theory can hardly be applicable, an equivalent depth of about 11 cm would be required. The equivalent depths for the first three modes (Nava and Ripa, private communication) are 45, 14 and 6.6 cm, respectively, so the best fit is to the second mode. Also this mode has a zero crossing in displacement around 400 m, which fits Fig. 15a better than any of the other modes.

The conclusion is that somewhere in the zone of poor data coverage (140–95°), a significant change in vertical displacement structure took place during the 1972 El Niño. The scatter diagram of all measurements along the equator of the 14°C isotherm level (Meyers 1979, Fig. 3) shows that the mean slope reverses at about 95°W and the range of scatter is much larger east of 100°W than it is to the west. This suggests that the change in vertical structure may occur near 100°W. The cause of the change may well be the shoaling of the thermocline toward the east, which reduces the thickness of the layer of water warmer than 14°C from about 200 m in the west to about 90 m at 95°W (Meyers, 1979, Fig. 3).

Whatever the cause, these observations show that to accurately reproduce subsurface changes in structure, a model based on a single mode perturbation to a resting ocean will not suffice. On the other hand, for sea-level (and hence surface current) changes, the first mode tends to dominate (Wunsch and Gill, 1976), so the single-mode model may be reasonably successful in reproducing those changes. Even so, details near the eastern boundary are likely to be poorly represented.

7. Summary

The bathythermograph data were adequate to describe the major changes in 1971–73 in two regions, the eastern boundary and in the central Pacific. At the eastern boundary, the changes in isotherm depth are very large, particularly in the zone within 10–15° of the equator. Similar changes occur further poleward, but the magnitudes are smaller and there is evidence that the changes occur a month or so later than at the equator. The surface temperature is usually higher than normal when the thermocline is depressed below its normal level. The changes in vertical structure near the equator are similar to those associated with the second baroclinic mode.

In the central Pacific, the major event in surface temperature was the warming in the second half of 1972. The thermocline at 170–160°W was actually above its normal level at this time, although two sections further west (148–158°W, 138–148°W) showed the thermocline was lower than normal there. The major anomalies in the 20°C isotherm displacement at 170–160°W in 1972–73 were the abnormally high levels in March–May and June–August 1973. The surface temperature was near normal in the first of these three-month periods, but below normal in the second. Thus, in contradistinction to the eastern boundary zone, there is *not* a good association between an anomalously warm surface and an abnormally low thermocline in this region.

Acknowledgments. I would like to thank Dr. Gary Meyers for supplying the BT data in a convenient format, and Mr. Julian Smith for the computer-drawn plots and the associated data analysis.

APPENDIX

Relation Between η and $\partial h/\partial z$ at the Surface for a Single Mode

Suppose the ocean has a small perturbation from the rest state and that this perturbation can be described in terms of one mode only. In other words (see Gill, 1982, Section 6.11), the dependent variables can all be written as products of a function of z and a function of the other dependent variables. One of the separation conditions is that the pressure perturbation is proportional to $\partial h/\partial z$ everywhere. It remains to show that the constant of proportionality is as in Eq. (1).

At the ocean surface, the momentum equations relating surface velocities (u, v) to the surface elevation η already have the shallow-water form. It follows that the remaining shallow-water equation, namely

$$H_e\left(\frac{\partial u}{\partial x} + \frac{\partial v}{\partial y}\right) + \frac{\partial \eta}{\partial t} = 0,$$

also applies with (u, v, η) interpreted as above and with H_e being the equivalent depth. The relation (1) now follows by comparing this with the incompressibility equation applied at the free surface. This equation can be written in the form

$$\frac{\partial u}{\partial x} + \frac{\partial v}{\partial y} + \frac{\partial^2 h}{\partial z \partial t} = 0.$$

REFERENCES

Anderson, D. L. T., and P. B. Rowlands, 1976: The role of inertia gravity and planetary waves in the response of a tropical ocean to the incidence of an equatorial Kelvin wave on a meridional boundary. *J. Mar. Res.*, **34**, 295–312.

Austin, T. S., 1960: Oceanography of the east central equatorial Pacific as observed during the expedition EASTROPIC. *Fish. Bull. Fish Wildlife Serv.*, **168**, 257–282.

Barnett, T. P., and W. C. Patzert, 1980: Scales of thermal variability in the tropical Pacific. *J. Phys. Oceanogr.*, **10**, 529–540.

Bjerknes, J., 1966a: A possible response of the atmospheric Hadley circulation to equatorial anomalies of ocean temperature. *Tellus*, **18**, 820–829.

——, 1966b: Survey of El Niño 1957–58 in its relation to tropic Pacific Meteorology. *Inter-Amer. Trop. Tuna Comm. Bull.*, **12**, 62 pp.

——, 1969: Atmospheric teleconnections from the equatorial Pacific. *Mon. Wea. Rev.*, **97**, 162–172.

Cane, M., and E. S. Sarachik, 1979: Forced baroclinic ocean motions. III. The linear equatorial basin case. *J. Mar. Res.*, **37**, 355–398.

Chelton, D. B., 1981: Interannual variability of the California Current—physical factors. CalCOFI Rep., **22**, 34–48. [California Cooperative Fisheries Investigations].

Donguy, J. R., and C. Henin, 1978: Surface salinity fluctuations between 1956 and 1973 in the western South Pacific Ocean. *J. Phys. Oceanogr.*, **8**, 1132–1134.

——, and ——, 1980: Surface conditions in the eastern equatorial Pacific related to the intertropical convergence zone of the winds. *Deep-Sea Res.*, **27**, 693–714.

Enfield, D. B., 1981: El Niño–Pacific eastern boundary response to interannual forcing. *Resource Management and Environmental Uncertainty*, M. H. Glantz and J. D. Thompson, Eds. Wiley, Chap. 8.

——, and J. S. Allen, 1980: On the structure and dynamics of monthly mean sea-level anomalies along the Pacific coast of North and South America. *J. Phys. Oceanogr.*, **10**, 557–578.

Gill, A. E., 1975: Models of equatorial currents. *Numerical Models of Ocean Circulation*, Nat. Acad. Sci., Washington, DC, 181–203.

——, 1982: *Atmosphere-Ocean Dynamics*. Academic Press, 662 pp.

Halpern, D., 1980: A Pacific equatorial temperature section from 172°E to 110°W during winter-spring 1979. *Deep-Sea Res.*, **27**, 931–940.

Henin, C., and J. R. Donguy, 1980: Heat content changes within the mixed layer of the equatorial Pacific Ocean. *J. Mar. Res.*, **38**, 767–780.

Hickey, B., 1975: The relationship between fluctuations in sea level, wind stress and sea-surface temperature in the equatorial Pacific. *J. Phys. Oceanogr.*, **5**, 460–475.

Hires, R. I., and R. B. Montgomery, 1972: Navifacial temperature and salinity along the tracks from Samoa to Hawaii 1957–1965. *J. Mar. Res.*, **30**, 177–200.

Horel, J. D., and J. M. Wallace, 1981: Planetary-scale atmospheric phenomena associated with the Southern Oscillation. *Mon. Wea. Rev.*, **109**, 813–829.

Hurlburt, H. E., J. C. Kindle and J. J. O'Brien, 1976: A numerical simulation of the onset of El Niño. *J. Phys. Oceanogr.*, **6**, 621–631.

Huyer, A., 1980: The offshore structure and subsurface expression of sea-level variations off Peru 1976–1977. *J. Phys. Oceanogr.*, **10**, 1755–1768.

McCreary, J. P., 1976: Eastern tropical ocean response to changing wind systems with application to El Niño. *J. Phys. Oceanogr.*, **6**, 632–645.

Masuzawa, J., and K. Nagasaka, 1975: The 137°E oceanographic section. *J. Mar. Res.*, **33**, 109–116.

Meyers, G., 1979: Annual variation of the slope of the 14°C isotherm along the equator in the Pacific Ocean. *J. Phys. Oceanogr.*, **9**, 885–891.

O'Brien, J. J., A. Busalacchi and J. Kindle, 1981: Ocean models of El Niño. *Resource Management and Environmental Uncertainty*, M. H. Glantz and J. D. Thompson, Eds., Wiley, Chap. 7.

Philander, S. G. H., and R. C. Pacanowski, 1980: The generation and decay of equatorial currents. *J. Geophys. Res.*, **85**, 1123–1136.

Rasmusson, E. M., and T. H. Carpenter, 1982: Variations in tropical sea-surface temperature and surface wind fields associated with the Southern Oscillation/El Niño. *Mon. Wea. Rev.*, **110**, 354–384.

Robles, F., E. Alarcón and A. Ulloa, 1980: Water masses in the northern Chilean zone and their variations in a cold period (1967) and warm periods (1969, 1971–73). *Proceedings Workshop on the Phenomenon known as El Niño*, UNESCO, Paris, 284 pp.

Smith, R. K., 1978: Poleward propagating perturbations in currents and sea-levels along the Peru Coast. *J. Geophys. Res.*, **83**, 6083–6092.

Sugonihara, N., 1981: Propagation of coastal-trapped waves at low latitudes in a stratified ocean with continental shelf slope. *J. Phys. Oceanogr.*, **11**, 1113–1122.

White, W. B., and K. Hasanuma, 1980: Interannual variability in the baroclinic gyre. *J. Mar. Res.*, **38**, 651–672.

Wooster, W. S., and O. Guillen, 1974: Characteristics of El Niño of 1972. *J. Mar. Res.*, **32**, 387–404.

Wunsch, C., and A. E. Gill, 1976: Observations of equatorially-trapped waves in Pacific sea-level variations. *Deep-Sea Res.*, **23**, 371–390.

Wyrtki, K., 1975: El Niño—the dynamic response of the equatorial Pacific Ocean to atmospheric forcing. *J. Phys. Oceanogr.*, **5**, 572–584.

——, 1977: Sea-level during the 1972 El Niño. *J. Phys. Oceanogr.*, **7**, 779–787.

——, 1979: The response of sea-surface topography to the 1976 El Niño. *J. Phys. Oceanogr.*, **9**, 1223–1231.

——, G. Meyers, D. McLain and W. Patzert, 1977: Variability of the thermal structure in the central equatorial Pacific ocean. Rep. HIG-77-1, Hawaii Inst. Geophys. 75 pp.

——, E. Firing, D. Halpern, R. Knox, G. J. McNally, W. C. Patzert, E. D. Stroup, B. A. Taft and R. Williams, 1981: The Hawaii to Tahiti Shuttle Experiment. *Science*, **211**, 22–28.

Zuta, S., D. Enfield, J. Valdivia, P. Lagos and C. Blandin, 1980: Physical aspects of the 1972–3 El Niño phenomenon. *Proceedings Workshop on the Phenomenon Known as El Niño*, UNESCO, Paris, 284 pp.